

3-d chemical imaging using angle-scan nanotomography in a soft X-ray scanning transmission X-ray microscope

A.P. Hitchcock · G.A. Johansson · G.E. Mitchell ·
M.H. Keefe · T. Tyliszczak

Received: 23 July 2007 / Accepted: 3 April 2008 / Published online: 24 May 2008
© Springer-Verlag Berlin Heidelberg 2008

Abstract Three-dimensional chemical mapping using angle scan nanotomography in a soft X-ray scanning transmission X-ray microscope (STXM) has been used to investigate the spatial distributions of a low density polyacrylate polyelectrolyte ionomer inside submicron sized polystyrene microspheres. Acquisition of tomograms at multiple photon energies provides true, quantifiable 3-d chemical sensitivity. Both pre-O 1s and C 1s results are shown. The study reveals aspects of the 3-d distribution of the polyelectrolyte that were inferred indirectly or had not been known prior to this study. The potential and challenges for extension of the technique to studies of other polymeric and to biological systems is discussed.

PACS 68.37.Yz · 81.70.Tx · 82.35.Lr

1 Introduction

Three-dimensional *chemical* mapping using angle scan tomography in a soft X-ray scanning transmission X-ray microscope (STXM) with sample scanning has recently been

developed [1–3]. To date we have applied it to quantitative chemical mapping in three dimensions of fully hydrated biological and polymer systems using the so called ‘water window’—i.e., taking advantage of the high transparency of water and glass just below the onset of their strong O 1s absorption signals. Previous angle-scan tomography in full field microscopy [4, 5] and STXM with zone plate scanning [6] has emphasized working at cryo temperatures (which is advantageous, especially for biological samples) but has only been carried out at a single photon energy, thereby providing mostly density, and only limited chemical contrast. Acquisition of tomograms at multiple photon energies allows access to quantifiable chemical information contained in the near edge X-ray absorption fine structure (NEXAFS) signal [7] and thus provides true 3-d chemical mapping. Here we describe progress towards the latter. In addition to presenting our approach, we illustrate its capabilities by mapping a low density polyacrylate polyelectrolyte ionomer in polystyrene microspheres inside an aqueous medium in a ~3 micron diameter glass microcapillary. Very recently we have obtained very thin walled carbon tubes [8] (courtesy of H. Bau and M. Schrlau, U. Pennsylvania) which have sufficiently low absorption that it is possible to examine low density organic samples at the C 1s edge. Our first results from STXM tomography measurements at the C 1s edge are reported.

2 Experimental

2-d and 3-d X-ray imaging and spectroscopy were carried out using the soft X-ray (200–600 eV) scanning transmission X-ray microscope at the polymer STXM microscope on beamline 5.3.2 at the Advanced Light Source [9, 10]. Image sequences (2 images in the pre-O1s study and 23 im-

A.P. Hitchcock (✉) · G.A. Johansson
BIMR, McMaster, Hamilton, L8S 4M1, Canada
e-mail: aph@mcmaster.ca

G.E. Mitchell
Analytical Science Dow Chemical, Midland, MI 48667, USA

M.H. Keefe
Dow Latex, Dow Chemical, Midland, MI 48674, USA

T. Tyliszczak
Advanced Light Source, LBNL, Berkeley, CA 94720, USA

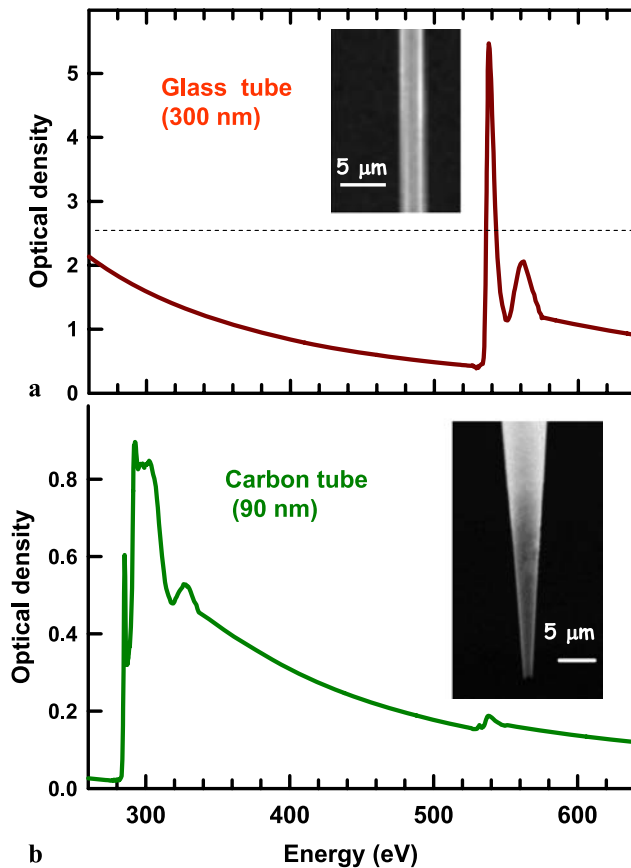


Fig. 1 (a) Optical density spectrum in the 260–640 eV range of thin walled (~ 150 nm) glass. The signal above 528 eV is measured, while that below 525 eV is taken from tabulated cross-sections [12]. The dashed line indicates the OD at which spectral distortions from absorption saturation effects typically appear in STXM 5.3.2. (b) Optical density spectrum in the 260–640 eV range of thin walled (~ 45 nm) carbon tubes. Even though the C 1s spectrum is highly structured and graphite-like, the low absorbance allows measurements at the C 1s edge

ages in the C 1s study) were measured at a fine mesh of angles (60 at O 1s, 50 at C 1s) in an angle scan computed tomography experiment. The resulting 4-dimensional (4-d) data set— $I(x, y, E, \theta)$ —was used to generate quantitative 3-d maps of the chemical species present in the sampled volume.

For the O 1s study, 3–5 μm diameter, thin-walled (150–200 nm) glass capillaries were used to hold the sample and keep it hydrated. For the C 1s study, a carbon tube with 45 nm walls (thickness as measured by its X-ray absorption) and internal diameter of 2–3 μm in the region of the sample was used. These latter tubes, kindly supplied by Prof. Bau, were fabricated [8] by depositing carbon inside a quartz micropipette via chemical vapor deposition (CVD) with argon/methane (3/2 mix) gas at 900 deg C. The carbon tube was then exposed by wet etching the tip of the micropipette with 5:1 HF.

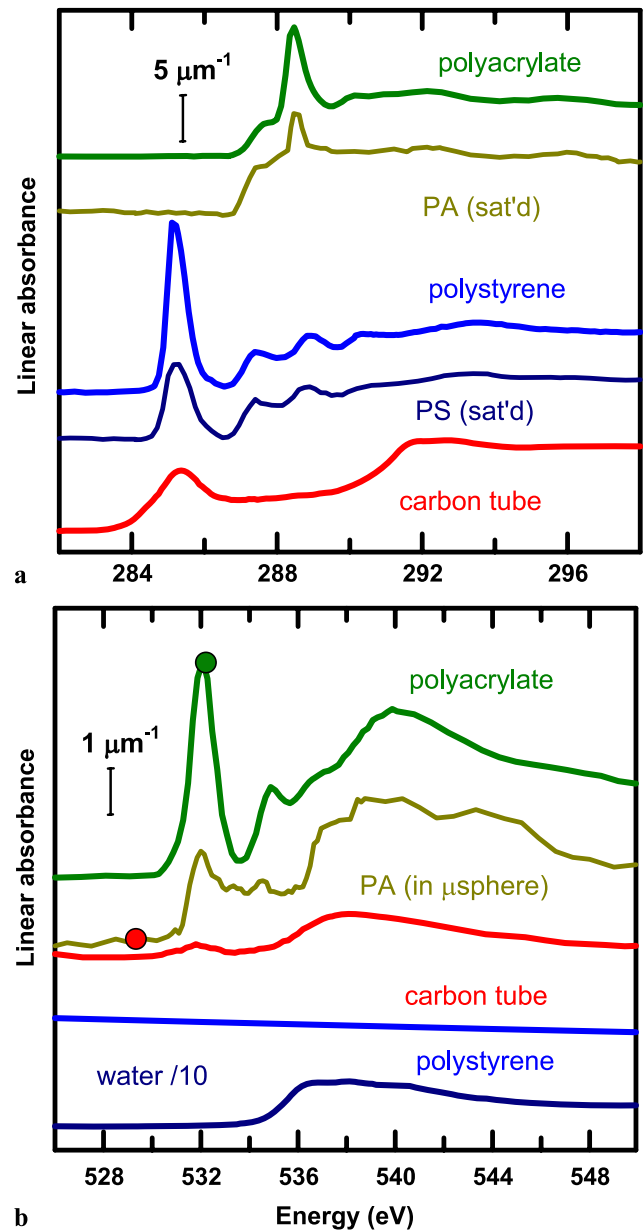


Fig. 2 (a) Comparison of the C 1s spectra of polyacrylate (PA), polystyrene (PS) and the carbon tube on a linear absorbance scale (optical density per nm thickness). Two sets of data for PA and PS are indicated, unsaturated and that extracted from spectra measured from the sample in the carbon tube. The spectrum of the carbon tube was subtracted from the spectrum of the center of the microspheres to produce a PS (sat'd) spectral curve similar to that of the unsaturated spectrum in the lower OD regions. Weighted spectra of both PS (sat'd) and the carbon tube were subtracted from the spectrum of the edges of the microspheres to produce the PA (sat'd) spectrum, again using matching to the spectral shape of the unsaturated PA spectrum in the lower OD regions as a guide to optimizing the spectral stripping process. (b) Comparison of the O 1s spectra of PA, PS, carbon tube, and water. The PA (in μsphere) spectrum is that from an O 1s spectral measurement of the same sample used for the C 1s tomographic study

Two classes of hollow polystyrene microspheres were investigated. Both were obtained as polymer colloidal dispersions in water with 30% polymer solids. For the O 1s study, the polystyrene microspheres were comprised of a rigid polystyrene (PS) shell which contained pores and a polyacrylate (PA) water solution dispersed between the core and serum phase. After drying, the water evaporates through the shell resulting in polystyrene microspheres of approximately 1 micron outer diameter, with the polyacrylate on the inner surface of the microspheres and the surrounding matrix. For the C 1s study, the polystyrene microspheres were comprised of a rigid polystyrene (PS) shell which was continuous (nonporous) and a polyacrylate (PA) water solution confined to the particle interior. After drying, the water evaporated through the shell resulting in hollow microspheres of approximately 0.75 micron outer diameter, with the polyacrylate on the inner surface of the shell. The polymer colloidal dispersions were diluted ten fold (for the C 1s study) or 10^4 -fold (for the O 1s sample) with distilled de-ionized water and then introduced into the capillary either from the top using a microsyringe (O 1s), or from the tip by capillarity (C 1s). For the O 1s study, both ends of the capillary were then sealed with silicone grease, and the sample was recorded with the capillary completely filled with water, which was retained throughout the measurements. For the C 1s study, only the top of the tube was sealed, leaving a very fine $\sim 1 \mu\text{m}$ hole at the tip partly open. Because of the inability to seal the bottom of the capillary, the water evaporated in the very initial stages of recording the C 1s data set, and thus this sample was mostly dry.

3 Results

Figure 1 presents the soft X-ray absorption spectrum (250–700 eV) of the two capillaries we have used in this work. The glass spectrum is that for a total path length of 300 nm, while the carbon spectrum is that for a total path length of 90 nm, in each case corresponding to twice the wall thickness of the actual capillaries used in these measurements. STXM images of the two types of capillaries are presented as inserts. Even in the C 1s region, where one would expect challenges due to the highly structured spectral response, the carbon capillary has considerable advantages over our current glass capillaries, with respect to lower total absorption. In particular, since X-ray absorption saturation effects occur in the STXM5.3.2 at ~ 2.5 OD units (and often lower in the C 1s region), the strong absorption by the glass gives major problems for the use of glass capillaries in the C 1s region. The weak O 1s signal in the carbon tube is residual silica. Prior to use of the carbon tubes, our lowest energy for tomography studies was only 340 eV, despite efforts to thin the capillary walls by HF etching and other means.

Figure 2 presents the spectral basis for chemical mapping in the polyacrylate–polystyrene–water–capillary system. Even though the carbon tube enables C 1s regime studies, the total path length of polystyrene (PS) in the walls of the microspheres is either 200 nm (1 sphere) or 400 nm (spheres) depending on whether the X-ray path goes through one or two balls. This leads to absorption saturation which clips the intensity of the strong C 1s $\rightarrow \pi_{\text{C}=\text{C}}^*$ peak at 285 eV. Thus, while there is excellent spectral contrast in the correct (i.e., unsaturated) spectra, the absorption saturation in the actual sample reduces the chemical contrast considerably, as the general effect of absorption saturation is a flattening of the spectral features. Despite this, there are still enough differences among the C 1s spectra of the chemical components—polyacrylate (PA), polystyrene (PS), and carbon tube—and retention of their characteristic spectral features to allow chemical mapping. For the PA, the characteristic C 1s $\rightarrow \pi_{\text{C}=\text{O}}^*$ peak is readily lost through radiation damage, and thus the accuracy of the PA mapping decreases as the integrated dose increases.

In the pre-edge O 1s region, PS, glass, and water absorbs only weakly, while polyacrylate has a characteristic O 1s $\rightarrow \pi_{\text{C}=\text{O}}^*$ peak at 532.2 eV. Above 534 eV, there is extreme absorption saturation caused by the very high absorption of the glass capillary and water. Even so, a study measuring tomograms on (532.2 eV) and just below (530 eV) the polyacrylate peak, at the energies highlighted in Fig. 2b, provides the key information needed for quantitative 3-d mapping of all the polymer components, when combined with the known OD of PS, and the OD and thickness of the glass and water components. The basis for the polyacrylate-specific mapping is demonstrated in Fig. 3, which shows OD images in one of the angular orientations at the two energies, as well as the difference of them. While the set of 2 images in the pre-O 1s region is adequate to map the system, as has been described and evaluated in detail elsewhere [1], there are many advantages to performing the chemical mapping using a larger set of images. These include: more accurate quantitation; ability to sense, identify and map unexpected chemical components; and improvement in the statistical quality. Of course acquiring more information requires longer time, and, of even greater importance, increased radiation dose. In this system, the polyacrylate is particularly radiation sensitive, and it is clear over the course of both the O 1s and C 1s tomographic study there was radiation damage. Thus the speed of acquisition, number of energies, and number of angles all have to be balanced against acceptable amounts of radiation damage.

Figure 4 shows an example of the C 1s based quantitative chemical analysis for one sample orientation in the C 1s tomographic study. The analysis is not fully optimized in several respects. First, the “tube” map is highly structured and has a uniform signal only in the region devoid of the microspheres, whereas, in an ideal analysis, it should look like

Fig. 3 (a) Optical density image at 530 eV. (b) Optical density image at 532 eV of the same orientation. (c) Difference of (a) and (b), which images the polyacrylate. Note the optical density gray scales

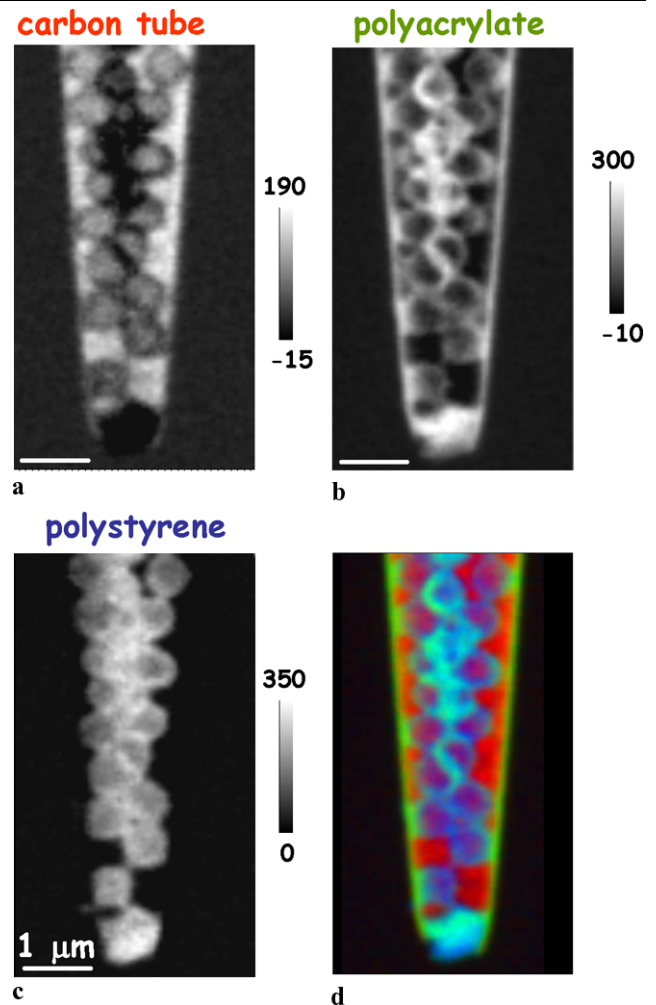
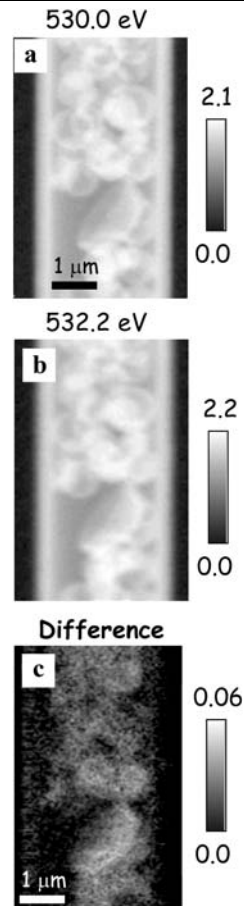


Fig. 4 Component maps for (a) carbon tube; (b) polyacrylate; (c) polystyrene derived from a fit to a C 1s image sequence (282–306 eV, 23 energies) at one angle, using the PA (sat'd), PS (sat'd) and carbon tube reference spectra plotted in Fig. 2. The gray scales are thickness in nm. (d) Color coded composite where the red maps carbon tube, green maps polyacrylate, and blue maps the polystyrene. The intensity of each color at any pixel is proportional to the amount of that component in the column traversed by the X-ray beam. Each color is rescaled independent of the other two

the tip of the tube in the insert to Fig. 1b. This is an effect of errors in the PS and PA reference spectra used for the fitting. Such spectra cannot be simply the optimized spectra of the pure materials because of absorption saturation. However, the degree of spectral distortion depends on the path length, and thus it is unlikely that any single distorted spectrum will fit at all thicknesses. Based on the current understanding that these hollow latex particles were comprised of a continuous shell, we did not expect the polyacrylate signal to be very strong outside the microspheres. However, the fitting suggests a layer of polyacrylate at the edge of the tube. The polyacrylate signal in the interior of the microspheres is as expected, since it is known that the PA material collapses onto the inner surfaces of the PS microspheres when it dries out [11]. Further analysis is needed to complete the workup of this tomographic data set and will be reported elsewhere. Also, we note that the sample is not optimum with regard to the scientific goal of the study, since it is dry rather than wet. It dried out early in the acquisition period because the tip of the carbon tube was not sealed. Attempts to date to seal the tip have resulted in broken tips. If the water was present, the chemical contrast would be further reduced due to the absorption by the water, but simulations suggest that the path length is still sufficiently short for penetration of some X-rays in the C 1s region.

Figure 5 presents 3-d visualizations of the microspheres based on the 2-energy data set recorded below the O 1s edge [1]. Figure 5a is a three-dimensional rendering of the combined chemical maps of the glass capillary, the PS (grey), and the polyacrylate (blue, green). Figure 5b is an alternate rendering of the region at the top of the sampled zone, while Fig. 5c presents an expansion of the lower zone. The particles have a dense shell comprised of predominately PS and a lower density core comprised of polyacrylate containing material. From standard electron microscopy analysis of the dried particles [11] the shell structure is known to be porous. Although some polyacrylate signal was detected outside of the microspheres, it was much less than expected, probably because the serum containing the particles was highly di-

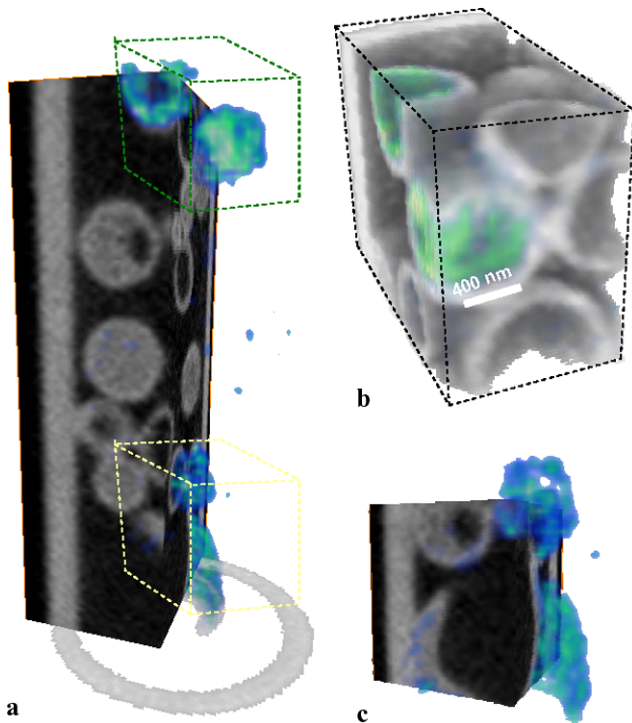
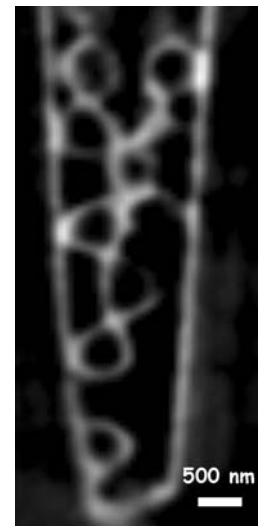


Fig. 5 3-d visualization of the sample structure from the two-energy O 1s tomography data set. **(a)** A cut through the whole volume, with the gray scale indicating both the PS and glass components, and the blue/green colorization indicating two density levels of the polyacrylate. **(b)** Expanded area of the upper box, using a different view and rendering. **(c)** Expanded view of the lower box

luted to assist introduction of the spheres into the capillary. Inside the microspheres, the distribution of the polyacrylate phase was found to be quite varied, with some spheres being completely and uniformly filled, others with only a small amount lining the inner surfaces (either uniformly or nonuniformly), and still others completely empty, either due to leakage through the PS walls, or in some cases, the presence of a uniform density of PS throughout the whole sphere [1]. This suggests that the shell structure is variable across particles. These measurements have provided the first direct evidence of nonuniform distributions of the polyacrylate phase in the particle core.

Figure 6 presents a cut through the center of a tomographic reconstruction of the set of polyacrylate component maps derived from the set of C 1s image sequences (282–306 eV; 0–120°). We caution that the analysis is not fully optimized, either in terms of the spectral fitting or precise alignment of the maps. In particular, there is most likely false fitting of the wall of the carbon tube by the absorption-saturation distorted polyacrylate reference spectrum. However, comparison of this slice to the 2-d projection of the polyacrylate component map in Fig. 4 nicely illustrates the better visualization the tomography provides.

Fig. 6 Slice through middle of the tomographic reconstruction of the polyacrylate component map derived from the C 1s image sequence measurements from 0–120°



4 Summary

Three-dimensional chemical mapping using angle scan tomography in a soft X-ray scanning transmission X-ray microscope (STXM) with sample scanning has been developed and demonstrated at both the O 1s and C 1s edges. It has been used to investigate the structure of two different polystyrene microspheres containing low density polyacrylate polyelectrolyte ionomers. The study reveals aspects of the 3-d distribution of the polyelectrolyte that were inferred indirectly or had not been known prior to this study. With further improvements in the experimental techniques and improved automation of the data processing, this promises to be a useful method for the analysis of soft materials and biological samples. For the latter, cryo-samples are needed to prevent sample degradation. This will require major modifications to existing STXM designs for practical implementation.

Acknowledgements We thank Michael Schrlau and Haim Bau for providing the carbon nanopipettes. We thank Daniel Hernández Cruz for assistance. We thank David Kilcoyne for his contributions to developing and maintaining the STXM5.3.2 microscope and Carolyn Larabell, Mark LeGros, and Wei-Wei Gu at the National Center X-ray Tomography (NCXT) for valuable discussions on tomography. Research supported by NSERC, Canadian Foundation for Innovation, and the Canada Research Chair program. The Advanced Light Source is supported by the Director, Office of Energy Research, Office of Basic Energy Sciences, Materials Sciences Division of the U.S. Department of Energy, under Contract No. DE-AC03-76SF00098.

References

1. G.A. Johansson, T. Tylliszczak, G.E. Mitchell, M.H. Keefe, A.P. Hitchcock, *J. Synchrotron Radiat.* **14**, 395–402 (2007)
2. G.A. Johansson, J.J. Dynes, A.P. Hitchcock, T. Tylliszczak, G.D.W. Swerhone, J.R. Lawrence, *Proc. SPIE* **6318**, 6318–11 (2006)

3. G.A. Johansson, J.J. Dynes, A.P. Hitchcock, T. Tylicszak, G.D. Swerhone, J.R. Lawrence, *Microsc. Microanal.* **12**(S2), 1412–1413 (2006)
4. D. Weiß, G. Schneider, B. Niemann, P. Guttman, D. Rudolph, G. Schmahl, *Ultramicroscopy*, **84**, 185–197 (2000)
5. C.A. Larabell, M.A. Le Gros, *Mol. Biol. Cell* **15**, 957–962 (2004)
6. Y. Wang, C. Jacobsen, J. Maser, A. Osanna, *J. Microsc.* **197**, 80–93 (2000)
7. J. Stöhr, *NEXAFS Spectroscopy*. Springer Tracts in Surface Science, vol. 25 (Springer, Berlin, 1992)
8. M.G. Schrlau, E.M. Falls, B.L. Ziober, H.H. Bau, *Nanotechnology* **19**(1), 015101 (2008)
9. T. Warwick, H. Ade, A.L.D. Kilcoyne, M. Kritscher, T. Tylicszak, S. Fakra, A.P. Hitchcock, P. Hitchcock, H.A. Padmore, *J. Synchrotron Radiat.* **9**, 254–257 (2002)
10. A.L.D. Kilcoyne, T. Tylicszak, W.F. Steele, S. Fakra, P. Hitchcock, K. Franck, E. Anderson, B. Harteneck, E.G. Rightor, G.E. Mitchell, A.P. Hitchcock, L. Yang, T. Warwick, H. Ade, *J. Synchrotron Radiat.* **10**, 125–136 (2003)
11. E. Beach, M. Keefe, W. Heeschen, D. Rothe, *Polymer* **46**, 11195–11197 (2005)
12. B.L. Henke, E.M. Gullikson, J.C. Davis, *At. Data Nucl. Data Tables* **54**, 181–342 (1993)